Aggregation in Nanobundles and the Effect of Diverse Environments on the Solution-Phase Photochemistry and Photophysics of –Re(CO) 3 L + (L = 1,10-Phenanthroline, 2,2‘-Bipyridine)...

ARTICLE *in* INORGANIC CHEMISTRY · SEPTEMBER 2006

Impact Factor: 4.76 · DOI: 10.1021/ic060266s · Source: PubMed

Inorg. Chem. **2006**, *45*, 6666–6677

Aggregation in Nanobundles and the Effect of Diverse Environments on the Solution-Phase Photochemistry and Photophysics of $-Re(CO)_3L^+$ (L = 1,10-Phenanthroline, 2,2′-Bipyridine) Pendants Bonded to Poly(4-vinylpyridine)

Ezequiel Wolcan,[||] Mario R. Feliz,[§] Jose L. Alessandrini,[‡] and Guillermo Ferraudi*[,†]

Radiation Laboratory, Notre Dame, Indiana 46556-0579, INIFTA and Departamento de Física, Facultad de Ciencias Exactas, UNLP, Casilla de Correo 67, (1900) La Plata, República Argentina, INIFTA, Casilla de Correo 16, Sucursal 4, (1900) La Plata, Argentina, and INIFTA, Casilla de Correo 16, Sucursal 4, (1900) La Plata, Argentina

Received February 15, 2006

The UV–vis spectroscopy and photochemical properties of $\{(vpy\text{-}[Re(CO)_3(2,2'\text{-}bpy)])_m(vpy\text{-}[Re(CO)_3(phen)])_n(vpy)_p\}\text{-}(CF_3SO_3)_{m+n}\}$, vpy = 4-vinylpyridine, $m = 131$, $n = 131$ or $m = 200$, $n = 150$, and $m + n + p = 600$, were investigated in solution phase. The polymers exist in solution as aggregates of polymer strands with radii as large as $\sim 10^2$ nm. Given the size of the poly-vpy backbone, the aggregates must contain a large number of strands. The luminescence spectrum exhibits a strong resemblance to the emission spectrum of $\{(vpy\text{-}[Re(CO)_3(phen)])_{200}\text{-}(vpy)_{400}\}(CF_3SO_3)_{200}$. The existence of Re(I) chromophores in diverse environments was shown by the intrinsic kinetics of the luminescence, the decay kinetics of the MLCT excited states observed by time resolved-absorption spectroscopy, and the quenching of the luminescence by various quenchers. Redox reactions of the MLCT excited states with the quenchers were responsible for the luminescence quenching. While static quenching resulted when Cu(II) and Fe(III) EDTA complexes were the quenchers, a dynamic quenching resulted with $Fe(CN)_6^{4-}$ or 2,2′,2″-triethanolamine, TEOA. The photochemical and photophysical properties of the mixed-pendant polymers have been discussed in terms of arrays of MLCT excited states whose energies are determined by the diverse environments of the Re(I) chromophores. Conversions (with and without radiation) of the upper-energy MLCT excited states to the ground state and lower-energy MLCT excited states and the latter excited state to the ground state account for the experimental results.

Introduction

Numerous studies have been concerned with thermal and photochemical reactions of inorganic polymers in the solid state and solution phase. Interest in their photochemical and photophysical properties is driven by their potential applications in catalysis and optical devices.[1−12] The properties in the solution phase of the polymers I and II were investigated in previous works.[1,9,12]

* To whom correspondence should be addressed. E-mail: ferraudi.1@ND.EDU.
[†] Notre Dame.
[‡] INIFTA and Departamento de Física, Facultad de Ciencias Exactas. Member of CICPBA.
[§] INIFTA. Member of CICPBA.
[||] INIFTA. Member of CONICET.

(1) Wolcan, E.; Ferraudi, G. *J. Phys. Chem. A* **2000**, *104*, 9281.
(2) Jones, W. E.; Hermans, L. Jr.; Jiang, B. In *Multimetallic and Macromolecular Inorganic Photochemistry*; Ramamurthy, V., Schanze, K. S., Eds.: Marcel Deker Inc.: New York, 1999; Vol. 4, Chapter 1.
(3) Ogawa, M. Y. In *Multimetallic and Macromolecular Inorganic Photochemistry*; Ramamurthy, V., Schanze, K. S., Eds.; Marcel Deker Inc.: New York, 1999; Vol. 4, Chapter 3.
(4) Stufkens, D. J.; Vlček, A. Jr. *Coord. Chem. Rev.* **1998**, *177*, 127 and references therein.
(5) Smith, G. D.; Maxwell, K. A.; DeSimone, J. M.; Meyer, T. J.; Palmer, R. A. *Inorg. Chem.* **2000**, *39*, 893.
(6) Petersen, J. D. In *Supramolecular Photochemistry*; Balzani, V., Ed.; Reidel: Dordrecht, The Netherlands, 1987; p 135.
(7) Balzani, V.; Scandola, F. In *Supramolecular Photochemistry*; Ellis Harwood: Chichester, U.K., 1991; p 355.
(8) Kaneko, M.; Tsuchida, E. *J. Polym. Sci.* **1981**, *16*, 397.
(9) Wolcan, E.; Feliz, M. R. *Photochem. Photobiol. Sci.* **2003**, *2*, 412.
(10) Wolcan, E.; Ferraudi, G.; Feliz, M. R.; Gomez, R. V.; Mickelsons, L. *Supramol. Chem.* **2003**, *15*, 143.
(11) Feliz, M. R.; Ferraudi, G. *Inorg. Chem.* **2004**, *43*, 1551.
(12) Wolcan, E.; Alessandrini, J. L.; Feliz, M. R. *J. Phys. Chem. B* **2005**, *109*, 22890.

10.1021/ic060266s CCC: $33.50
Published on Web 07/26/2006

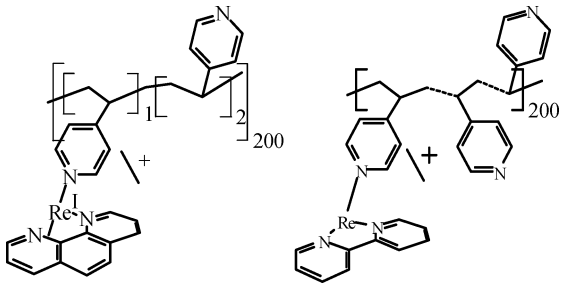

(I) (II)

(CO ligands coordinated to Re(I) were omitted for clarity.)

These polyelectrolytes have nearly 200 groups, −Re^{I}(CO)$_3$(phen)$^+$ (phen = 1,10-phenanthroline) or −Re^{I}(CO)$_3$(2,2′-bpy)$^+$ (2,2′-bpy = 2,2′- bipyridine) bonded to poly-(4-vinylpyridine), (vpy)$_{600}$, with an average of 600 4-vinylpyridine units.

Marked differences were found between the photochemical and photophysical properties of polymers I and II and those of the related monomeric complexes, pyRe^{I}(CO)$_3$L$^+$ (L = phen, 2,2′-bpy). The main cause of these differences is the photogeneration of MLCT excited sates in concentrations that are much larger when −Re^{I}(CO)$_3$L$^+$ chromophores are bound to (vpy)$_{600}$. This is the photophysical result of Re(I) chromophores being crowded in strands of a polymer instead of being homogeneously distributed through solutions of a pyRe^{I}(CO)$_3$L$^+$ complex. The recently communicated association of several hundred strands of II in nearly spherical aggregates also contributes to the crowding of chromophores in small spaces in the solution, where the interaction between excited states becomes appreciable.[12]

The interaction between the Re(I) to phen charge-transfer excited states, ^{3}MLCT, makes the photophysical properties of the pendant chromophores in I deviate from those of pyRe^{I}(CO)$_3$(phen)$^+$. The annihilation of two ^{3}MLCT excited states, Scheme 1, forms chromophores in the ground state and intraligand, IL, electronic state. The latter being an excited state with a higher energy than the ^{3}MLCT excited state. In contrast to the ^{3}MLCT excited states, the ^{3}IL excited states oxidize organic solvents (e.g., CH_3OH).

In a peralkylated polymer, III in Scheme 2, the 350 nm irradiation of the Re(I) chromophores induces charge-transfer processes between the chromophores.[11] This process is in contrast with the intrastrand energy transfers that occur during the irradiation of I.[1]

The ^{3}MLCT excited states and charge-separated intermediates in III react with neutral (e.g., 2,2′,2″-triethanolamine) or anionic electron donors (e.g., SO_3^{2-} and I^-). The reactions of the anionic electron donors with the excited state of these polyelectrolytes are more efficient than similar reactions with the excited state of pyRe(CO)$_3$L$^+$. Similar photochemical and photophysical observations have been made with a polymer, II, containing −Re(CO)$_3$(2,2′-bpy)$^+$ chromophores.

Since excited-state−excited-state interactions, resulting from the polymer's morphology, have such a large influence on the photophysical and photochemical processes, polymers with more than one type of chromophore are expected to exhibit more varied interactions than those described for polymers I−III. Also, the specific environments that the strands and aggregates of strands create for the Re(I) chromophores will affect their photochemical properties (e.g., the lifetime of the MLCT excited states). These phenomena were investigated in this work with polymers IV and V.

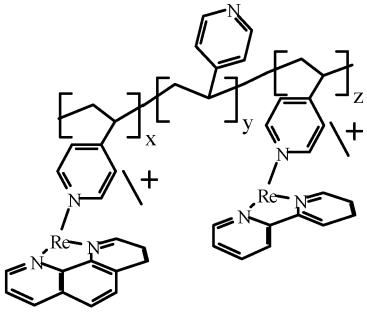

((IV) x = z = 131, y = 338 (V) x = 150, y = 250, z = 200. CO ligands coordinated to Re(I) were omitted for clarity.)

The two different pendants simultaneously bound to (vpy)$_{600}$ (i.e., −Re(CO)$_3$(phen)$^+$ and −Re(CO)$_3$(2,2′-bpy)$^+$) have similar redox properties, but there are differences in the energy and nature of their excited states. These differences made them suitable compounds to examine these phenomena.

Experimental Section

Light-Scattering Intensity Measurements. The time correlation $G(q,t)$ of the light-scattering intensity was measured at 90° with a goniometer, ALV/CGS-5022F, with a multiple-τ digital correlator, ALV-5000/EPP, covering a 10^{-6}−10^3 s time range. The light source was an helium/neon laser with a wavelength of 633 nm operating at 22 mW. All the measurements were carried out at room temperature.

$G(q,t)$ is measured at a given wave vector, $q = (4\pi n/l)\sin(\theta/2)$, where n is the refractive index of the medium, l is the wavelength in a vacuum, and θ is the scattering angle. Under the homodyne conditions valid for the present system, the measured $G(q,t)$ is related to the desired normalized electric-field correlation function, $g(q,t)$ (eq 1).

$$G(q,t) = A_\infty[1 + f^*|\alpha g(q,t)|^2] \quad (1)$$

In eq 1, f^* is an instrumental factor, α is the fraction of the total scattered intensity, $I(q)$, resulting from fluctuations in the optical polarizability with correlation times longer than 10^{-6} s, and A_∞ is the baseline measured at long delay times. The incident laser beam was polarized perpendicular to the scattering plane. $I(q)$ is the isotropic component of the light-scattering intensity caused by density and concentration fluctuations with the former being, in principle, much faster.

The characteristic relaxation parameters were extracted with the inverse Laplace transformation (ILT) of the measured $G(q,t)$

Scheme 1 [a]

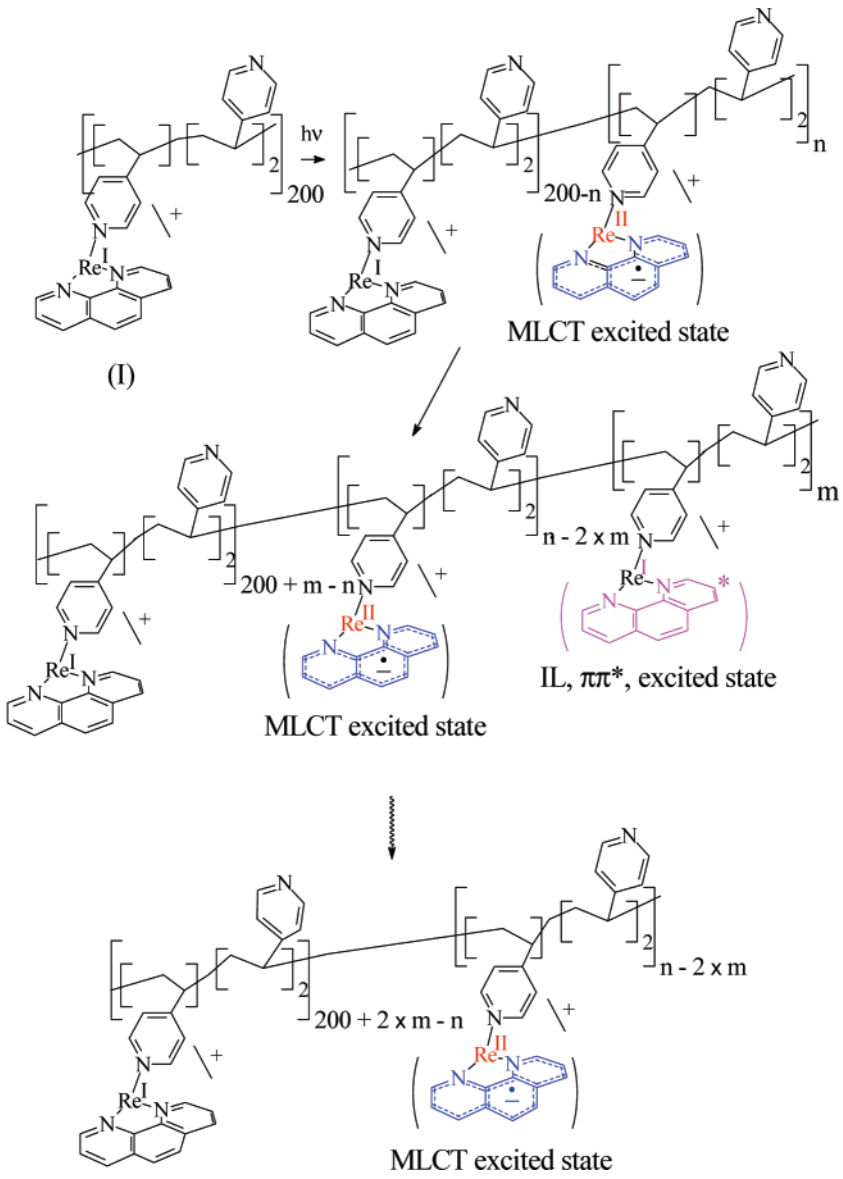

[a] CO ligands coordinated to Re(I) were omitted for clarity.

(eq 2) under the assumption of a superposition of exponentials.

$$\left\{\frac{\left[\frac{G(q,t)}{A_\infty}\right]-1}{f^*}\right\}^{1/2} = \alpha g(q,t) = \int_{-\infty}^{\infty} L(\ln \tau_r)\, e^{-t/\tau_r}\, d(\ln \tau_r) \quad (2)$$

The Stokes−Einstein equation (eq 3) relates the hydrodynamics radius of the polymer, R_h, with the relaxation time, τ_r, where k_B is

$$R_h = k_B T q^2 \tau_r / 6\pi\eta \quad (3)$$

the Boltzmann constant, T is the absolute temperature, and η is the shear viscosity of the solvent in a low concentration regime. The relaxation times and radii at the maxima of the corresponding distributions are reported as mean values with the corresponding standard deviations of the mean. These values were obtained from the statistics of several independent experiments. Since all DLS measurements were carried out at a polymer concentration of 0.5 mg cm^{-3}, the reported hydrodynamic radii are apparent values. A study of the DLS dependence on polymer concentration is not within the scope of this work.

TEM. Transmission electron micrographs were recorded on a JEOL 100 CX electron microscope at an electron-acceleration voltage of 80 kV with a nominal point-to-point resolution of 3 Å. The photos were taken at an amplification of 20 000×.

Flash-Photochemical Procedures. Optical density changes occurring in a time scale longer than 10 ns were investigated with a flash photolysis apparatus described elsewhere.[13−15] In these experiments, 10 ns flashes of 351 nm light were generated with a Lambda Physik SLL-200 excimer laser or 1 ns flashes of 355 nm light were generated with a Continuum Powerlite Nd:YAG laser. The energy of the laser flash was attenuated to values equal to or less than 20 mJ/pulse by absorbing some of the laser light in solutions of $Ni(ClO_4)_2$ with appropriate optical transmittances, $T = I_t/I_0$, where I_0 and I_t are the intensities of the light arriving to and being transmitted from, respectively, the photolysis cell. The transmittance, $T = 10^{-A}$, was routinely calculated with the

(13) Feliz, M. R.; Ferraudi, G. *J. Phys. Chem.* **1992**, *96*, 3059.
(14) Feliz, M. R.; Ferraudi, G.; Altmiller, H. *J. Phys. Chem.* **1992**, *96*, 257.
(15) Guerrero, J.; Piro, O. E.; Wolcan, E.; Feliz, M. R.; Ferraudi, G.; Moya, S. A. *Organometallics.* **2001**, *20*, 2842.

Scheme 2 [a]

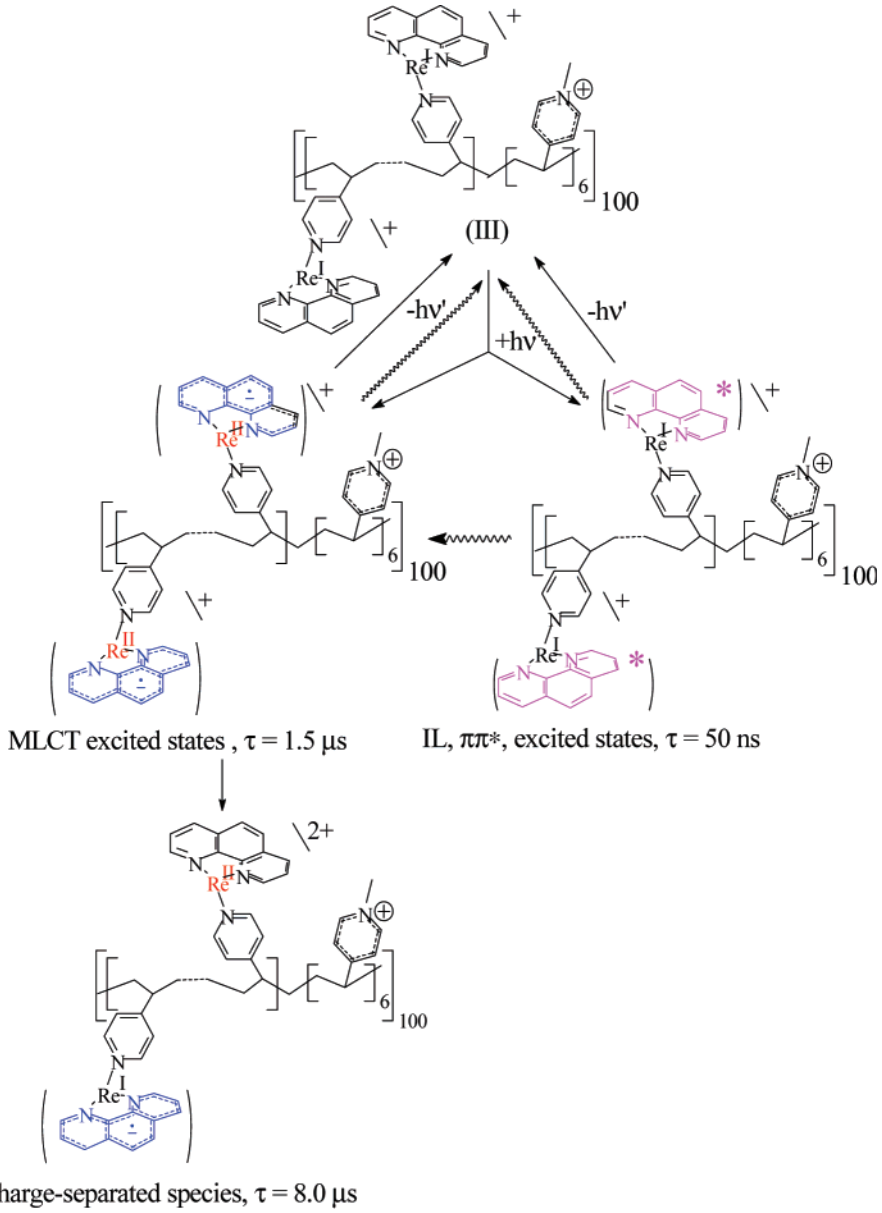

[a] CO ligands coordinated to Re(I) were omitted for clarity.

spectrophotometrically measured absorbance, *A*, of the solution. A right angle configuration was used for the pump and probe beams. Concentrations of the complexes were adjusted to provide homogeneous concentrations of photogenerated intermediates over the optical path, $l = 1$ cm, of the probe beam. To satisfy this optical condition, solutions were prepared with an OD equal to or less than 0.4 over the 0.2 cm optical path of the pump. Time-resolved fluorescence experiments were carried out with a PTI flash fluorescence instrument.[15] The excitation light was provided by a N_2 laser ($\lambda_{em} = 337$ nm, ca. 2 mJ/pulse) or by irradiation at 337 nm of suitable Exciton dyes ($\lambda_{em} = 350$ or 457 nm with a 0.2 ns pulse width and ca. 0.2 mJ/pulse). The concentrations of the complexes were adjusted to optical densities equal to or less than 0.05 for a 1 cm optical path at 350 nm. All the solutions used in the photochemical work were deaerated with streams of ultrahigh-purity N_2 before and during the irradiation.

Steady-State Irradiation. The luminescence of the Re(I) complexes was investigated in an SLM-Aminco-8100 interfaced to a Dell 333P microcomputer.[13] The spectra were corrected for differences in instrumental response and light scattering. Solutions were deaerated with O_2-free nitrogen in a gastight-apparatus before recording the spectra.

Pulse Radiolysis. Pulse radiolysis experiments were carried out with a model TB-8/16-1S electron linear accelerator. The instrument and computerized data collection for the time-resolved UV−vis spectroscopy and reaction kinetics have been described elsewhere in the literature.[16,17] Thiocyanate dosimetry was carried out at the beginning of each experimental session. The details of the dosimetry have been reported elsewhere.[16,18] The procedure is based on the concentration of $(SCN)_2^{\bullet-}$ radicals generated by the electron pulse in a N_2O-saturated 10^{-2} M SCN^- solution. In the procedure, the calculations were made with $G = 6.13$ and a extinction coefficient, ϵ, of 7.58×10^3 M^{-1} cm^{-1} at 472 nm, for the $(SCN)_2^{\bullet-}$ radicals.[16,18]

(16) Hug, G. L.; Wang, Y.; Schöneich, C.; Jiang, P.-Y.; Fessenden, R. W. *Radiat. Phys. Chem.* **1999**, *54*, 559.
(17) Buxton, G. V.; Greenstock, C. L.; Helman, W. P.; Ross, A. B. *J. Phys. Chem. Ref. Data* **1988**, *17*, 513.
(18) Feliz, M. R.; Ferraudi, G. *Inorg. Chem.* **1998**, *37*, 2806.

The doses produced in aqueous solutions $(2.0 \pm 0.1) \times 10^{-6}$ to $(6 \pm 0.3) \times 10^{-6}$ M concentrations of e^-_{sol}. In the experiments, solutions of the reactants were deaerated with streams of the O_2-free gases, N_2 or N_2O. To irradiate a fresh sample with each pulse, an appropriate flow of the solution through the reaction cell was maintained during the experiment.

The radiolysis of CH_3OH and CH_3OH/H_2O mixtures with ionizing radiation has been reported elsewhere in the literature.[19−21] These studies have shown that pulse radiolysis can be used as a convenient source of e^-_{sol} and $C^{\bullet}H_2OH$ radicals. The sequence of events in the radiolysis of these solvents is shown in eq 4.

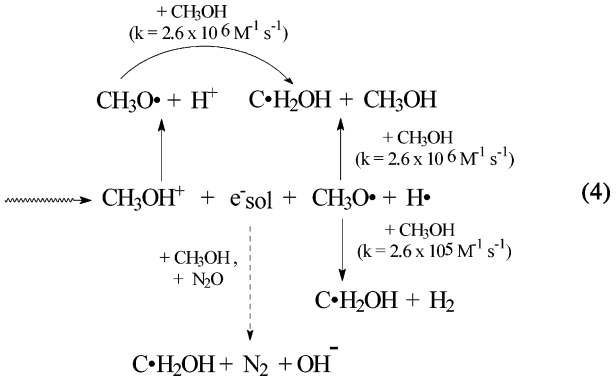

Because e^-_{sol} and $C^{\bullet}H_2OH$ have large reduction potentials (i.e., −2.8 V vs NHE for e^-_{sol} and −0.92 V vs NHE for $C^{\bullet}H_2OH$), they have been used for the reduction of coordination complexes and for the study of electron-transfer reactions. The yield of e^-_{sol} in CH_3OH ($G \approx 1.1$) is about a third of the G value in the radiolysis of H_2O ($G \approx 2.8$).[19] In solutions where e^-_{sol} was scavenged with N_2O,[21] the $C^{\bullet}H_2OH$ radical appears to be the predominant product (yield > 90%) of the reaction between CH_3OH and $O^{\bullet-}$.

Materials. $CF_3SO_3Re(CO)_3(2,2'\text{-bpy})$ and $CF_3SO_3Re(CO)_3(phen)$ were prepared and purified by a literature procedure that involves the reaction of $BrRe(CO)_3(2,2'\text{-bpy})$ or $BrRe(CO)_3(phen)$ with $AgCF_3SO_3$. $\{[(vpy)_2\text{-vpyRe}(CO)_3(2,2'\text{-bpy})](CF_3SO_3)\}_{200}$ was available from a previous work.[9] Aldrich's poly-$(4\text{-vpy})_{600}$, $(vpy)_{600}$, with M_w = ca. 6×10^4, was used without purification in the following preparations.

Preparation of $\{[(vpy)_{600}\text{-}[Re(CO)_3(2,2'\text{-bpy})]_{131}\text{-}[Re(CO)_3(phen)]_{131}(CF_3SO_3)_{262}\}$ (IV). The reaction of an equimolar mixture of $CF_3SO_3Re(CO)_3(2,2'\text{-bpy})$ and $CF_3SO_3Re(CO)_3(phen)$ with $(vpy)_{600}$, fw = 6×10^4, was used in the preparation of IV. In the synthesis of the derivatized polymer, a solution that contained 40 mg of $CF_3SO_3Re(CO)_3(2,2'\text{-bpy})$ and 41 mg of $CF_3SO_3Re(CO)_3(phen)$ in 50 mL of CH_2Cl_2 (1.38×10^{-4} mol of $-Re(CO)_3L$; 131 $-Re(CO)_3(2,2'\text{-bpy})$ groups and 131 $-Re(CO)_3(phen)$ groups per 600 py groups present in the $(vpy)_{600}$) was slowly added by being stirred into a solution containing 33.3 mg of $(vpy)_{600}$ (5.29×10^{-7} mol) in 25 cm^3 of CH_2Cl_2. The solution was refluxed overnight, and a yellow product precipitated. The mixture was rotatory evaporated to dryness, and the resulting solid was recrystallized by the slow addition of ethyl ether from CH_3CN. The resulting yellow complex was dried under vacuum at room temperature until a constant weight was obtained. Yield 90% (87 mg). Anal. Calcd for $Re_4C_{124}H_{36}N_{17}O_{24}S_4F_{12}$ as a minimum formula of IV: H, 2.90; C, 44.95; N, 7.25. Found H, 3.17; C, 44.79; N, 7.17.

Preparation of $\{[(vpy)_{600}\text{-}[Re(CO)_3(2,2'\text{-bpy})]_{200}\text{-}[Re(CO)_3(phen)]_{150}(CF_3SO_3)_{350}\}$ (V). A solution containing 23 mg of $CF_3SO_3Re(CO)_3(phen)$ in 50 mL of MeOH was slowly added to a vigorously stirred solution containing 33 mg of $\{[(vpy)_2\text{-vpyRe}(CO)_3(2,2'\text{-bpy})](CF_3SO_3)\}_{200}$ in 50 mL of MeOH. The resulting solution was refluxed overnight and then rotatory evaporated to dryness. The product was recrystallized by the slow addition of ethyl ether to a solution of the crude compound in CH_3CN. The resulting yellow complex was dried under vacuum at room temperature until a constant weight was obtained. Yield 86% (48 mg). Anal. Calcd for $Re_3C_{81}H_{63}N_{11}O_{18}S_3F_9$ as a minimum formula of V: H, 2.61; C, 42.06; N, 6.79. Found H, 2.96; C, 41.89; N, 6.71.

Gel Permeation Chromatography. In addition to the NMR and UV−vis absorption spectroscopies, the purity of the polymers was assessed by gel permeation chromathography in Sephadex LH-20. A standard protocol provided by Sephadex was followed for the preparation of the gel in methanol. The solutions of monomer and polymer Re compounds were made in methanol. The compounds or mixtures were loaded in the column and eluted with methanol. Tests of the chromatographic separation were made with solutions containing mixtures of monomeric and polymeric Re compounds. The large difference between the retention times of the monomeric and polymeric materials ensured their complete separation. Chromatographies of the polymers used in this work showed the absence of free monomeric contaminants.

Results

A symptom of the coordination of Re(I) groups to a polymeric backbone is a minor shift and a considerable broadening of the resonances in their NMR spectrum, Figure 1S. Although the NMR spectroscopy, UV−vis spectroscopy, communicated below, and GPC confirm the polymeric nature of compounds IV and V, the interpretation of their photophysical properties required knowledge of the polymers' morphologies. Results from these morphological studies are communicated next with results of the photophysical and photochemical experiments.

Dynamic Light Scattering (DLS). Solutions of polymer IV or V, ∼0.5 mg cm^{-3} in acetonitrile, at room temperature exhibited a bimodal spectrum of relaxation times, Figure 2S and Table 1S. The long-time distribution peak of IV with a maximum at 1.02 ± 0.04 ms was similar to those previously communicated for polymer II.[12] The short-time contribution consisted of two wide unresolved peaks covering the range of 0.01−0.1 ms, with maxima at 0.015 ± 0.002 and 0.060 ± 0.003 ms. The height of both peaks is less than 0.20 of the height of the long-time peak. The hydrodynamics radius calculated for polymer IV with the Stokes−Einstein equation were as follows: 221 ± 9, 3.3 ± 0.4, and 13.0 ± 0.7 nm.

The solution of polymer V also displayed a bimodal spectrum of relaxation times. While spectrum of polymer V resembles that of polymer IV, the long-time peak of the former polymer appears displaced to longer times relative to the peak in the spectrum of IV. A hydrodynamics radius (294 ± 5 nm) was calculated with the position of this maximum (1.37 ± 0.02 ms). The short-time peaks are located at 0.012 ± 0.002 and 0.065 ± 0.007 ms, with heights not

(19) Getoff, N.; Ritter, A.; Schworer, F. *Radiat. Phys. Chem.* **1993**, *41*, 797.
(20) Dorfman, L. M.; In *The Solvated Electron in Organic Liquids*; Gould, R. F., Ed.; Advances in Chemistry Series 50; American Chemical Society: Washington, DC, 1965; pp 36−44.
(21) Simic, M.; Neta, P.; Hayon, E. *J. Phys. Chem.* **1969**, *73*, 3794.

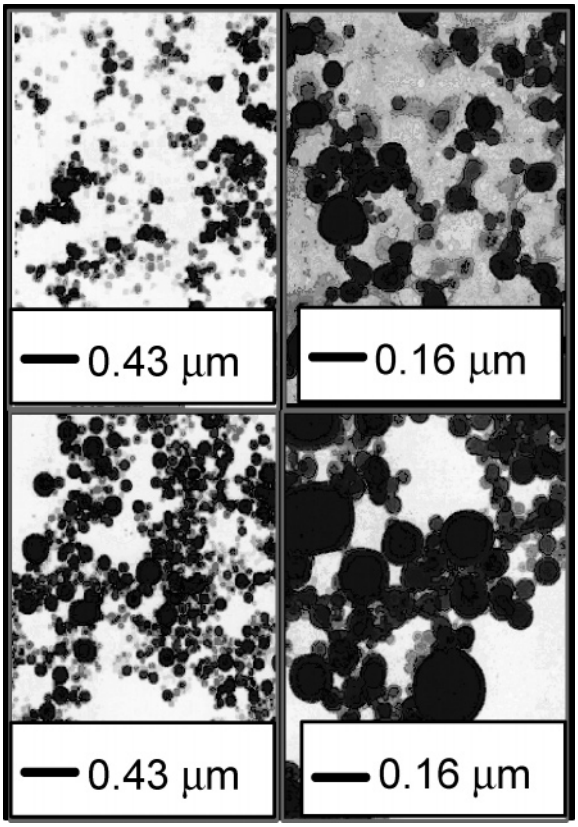

Figure 1. Transmission electron micrographs of the solvent cast films of IV (top) and V (bottom).

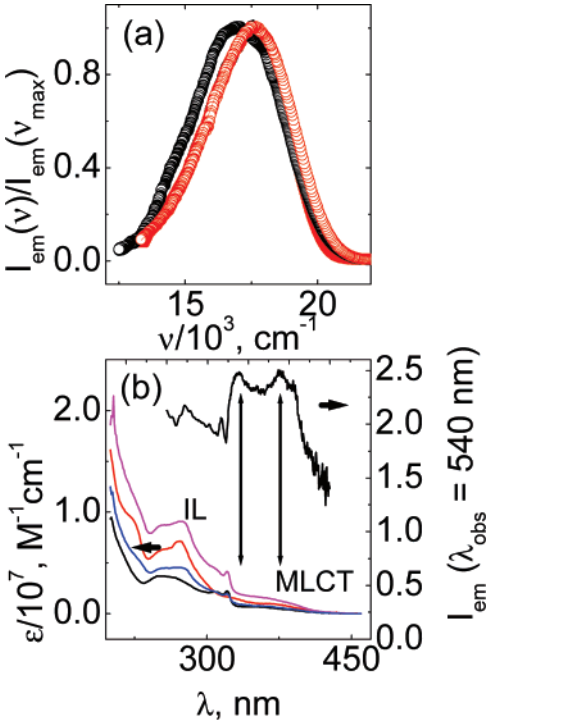

Figure 2. Comparison of the spectroscopic properties of $(vpy)_{600}$ polymers containing triscarbonyl Re(I) pendants. (a) Normalized emission spectra of I (○) II (○), IV (▼), and V (▲) in CH_3CN. The spectra of IV and V overlapped after they were normalized to the maximum emission intensity, $I_{em}(\nu_{max})$. (b) Absorption spectra (left axis) of (vpy) polymer with Re(I) pendants: I (red), II (black), IV (magenta), and V (blue). The excitation spectrum of V is plotted against the right axis.

higher than 0.10 of the long-time peak's height. The hydrodynamics radii calculated with them are as follows: 2.6 ± 0.5 and 14 ± 2 nm, respectively.

Solvent-Cast Films of the Polymers. The morphologies of polymers IV and V were also studied by transmission electron microscopy, TEM. Polymer films were obtained by room temperature evaporation of solutions of IV and V in acetonitrile. These polymer films were not stained with any chemicals, and the contrast of the image in the TEM photos (the observed shapes in Figure 1) can only originate from the Re(I) chromophores bound to $(vpy)_{600}$. The Re(I) complexes in polymer IV form aggregates of isolated nanodomains that are dispersed in the polymer-matrix film. The dimensions of the nanodomains are between 32 and 160 nm, and they are mainly spherical in shape. The nanodomains formed with polymer V are bigger than those formed by polymer IV (i.e., between 32 and 260 nm). It should be noted that the dimensions of the nanodomains of IV and V are considerably larger than the full stretch length of the polymers. Therefore, the nanodomains contain a considerable number of polymer molecules.

Luminescence. The emission spectra of the mixed-pendant polymers IV and V have identical band shapes with intensities proportional to the Re(I) load. Normalization of the spectra to the respective Re(I) loads made the bands indistinguishable, Figure 2a. This normalization also made the strong resemblance between the emission spectra of mixed-pendant polymers IV and V, on one side and the spectra of polymers I and II, containing only one type of Re(I) pendant, on the other side, evident. The normalized bands in the spectra of IV and V could almost be superimposed on the normalized band in the emission spectrum of the polymer I, containing only $-Re(CO)_3(phen)^+$ pendants. Few if any changes were observed in the emission spectra of IV and V when they were irradiated with monochromatic light in the following range of wavelengths: $250 \leq \lambda_{exc} \leq 450$ nm.

The excitation spectrum of polymer V, together with the absorption spectra of a number of polymers containing triscarbonylRe(I) pendants, is shown in Figure 2b. When the excitation spectrum of the mixed-pendant polymers were recorded, the emission was monitored near the maximum of the emission spectrum (i.e., ∼550 nm). The two most intense features in the excitation spectrum (i.e., 390 and 339 nm) correspond to wavelengths of the Re(I) to 2,2′-bpy and Re(I) to phen MLCT optical transitions of the Re(I) pendants. Narrow bands can be seen in the excitation and absorption spectra of all the $-Re(CO)_3(2,2'\text{-bpy})^+$-containing polymers; they appear at nearly the same position (i.e., ∼305 nm) in the excitation and absorption spectra. A related spectral feature in the spectrum of the $-Re(CO)_3(phen)^+$-containing polymers appears as a broad and less intense band positioned at approximately the same wavelength. The excitation spectrum shows additional contributions to the polymers' luminescence when they are irradiated below 300 nm (i.e., a spectral region corresponding to intraligand transitions of the 2,2′-bpy and phen ligands in the Re(I) chromophores).

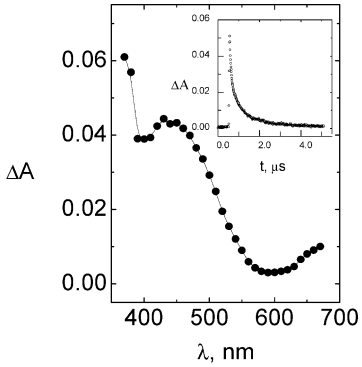

Figure 3. Difference absorption spectrum of the ^{3}MLCT excited states of the $-Re(CO)_3(phen)^+$ and $-Re(CO)_3(2,2'\text{-bpy})^+$ pendants in IV. The solutions of IV in CH_3CN contained a concentration of Re(I) chromophores of $[Re(I)] \approx 3.0 \times 10^{-4}$ M, and it was flash irradiated at 351 nm. The inset is a typical oscillographic trace revealing the biexponential decay of the absorbance at $\lambda_{ob} = 450$ nm.

Absorption Spectra of the Excited States. Solutions of the Re(I) polymers in deaerated CH_3CN were flash irradiated at 351 nm. The transient spectrum recorded ~30 ns after the irradiation has the spectral features, attributed to the ^{3}MLCT excited states of the $-Re(CO)_3(phen)^+$ and $-Re(CO)_3(2,2'\text{-bpy})^+$ chromophores, Figure 3. For example, the ^{3}MLCT excited-state spectrum in Figure 3 shows features observed in the excited-state spectrum of the pendants $-Re(CO)_3(phen)^+$ and $-Re(CO)_3(2,2'\text{-bpy})^+$ of polymers I and II, containing one or the other pendant (i.e., $\lambda_{max} = 440 \pm 5$ nm and $\lambda_{max} > 640$ nm).[1,9,11] Oscillographic traces (inset of Figure 3) were recorded at a given wavelength, λ_{ob}, within a 300−670 nm interval. They were fitted to a biexponential, $A_{0,1} \exp(-t/\tau_1) + A_{0,2} \exp(-t/\tau_2)$, where the order of magnitude of τ_1 and τ_2 are 10^{-7} and 10^{-6} s, respectively. While plots of $k_1 = 1/\tau_1$ versus λ_{ob} revealed a marked functional dependence on λ_{ob}, no such dependence was observed with the rate constant $k_2 = 1/\tau_2$, Figure 4. One interpretation of the preceding experimental observations is the presence of Re(I) chromophores in a diversity of environments within a polymer's aggregate.

Kinetics of the Luminescence. The kinetics of the luminescence decay was investigated as a function of the irradiation wavelength (i.e., $\lambda_{exc} = 266$, 308, or 351 nm) with solutions of Re(I) polymers IV and V in deaerated CH_3CN. Each oscillographic trace was recorded by following the decay of the luminescence at a given wavelength within an interval of wavelengths between 450 and 650 nm. These experiments revealed a biphasic decay of the luminescence which could be fitted, within the experimental error, to a biexponential function. The lifetimes of the two exponential terms have the same order of magnitude (i.e., 10^{-7} and 10^{-6} s) calculated in the preceding section for the biexponential decay of the MLCT excited-state absorption spectrum.

Excited-State Redox Reactions. To investigate the chemical behavior of chromophores in different environments, the polymers' luminescence was quenched with various compounds. EDTA complexes of Cu(II) and Fe(III) proved to be efficient quenchers of the luminescence of polymers IV and V. A decrease of the chromophores' luminescence with quencher concentration was observed in a range of quencher

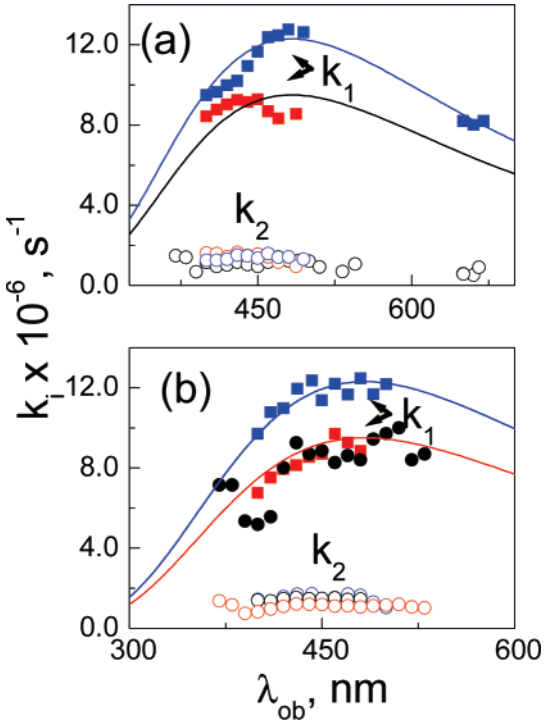

Figure 4. Dependence on λ_{ob} of the rate constants, k_1 (solid symbols) and k_2 (open symbols), calculated for the decay of the electronically excited $-Re(CO)_3(phen)^+$ and $-Re(CO)_3(2,2'\text{-bpy})^+$ pendants in the polymers IV (a) and V (b). Deaerated solutions of the polymers in CH_3CN contained concentrations of −Re(I) chromophores of $[Re(I)] \approx 1.0 \times 10^{-4}$ M, and they were flash irradiated at $\lambda_{exc} = 351$ (red), 308 (black), or 366 nm (blue).

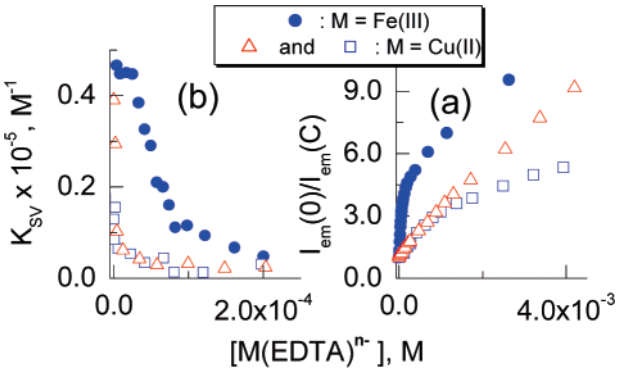

Figure 5. Stern−Volmer plots (a) showing the quenching of the luminescence of polymer IV with EDTA complexes. In experiments with $Cu(EDTA)^{2-}$, the concentrations of Re(I) chromophores were as follows: $[Re(I)] \approx 1.4 \times 10^{-4}$ M ($\lambda_{exc} = 410$ nm) (□) and $[Re(I)] \approx 1.4 \times 10^{-3}$ M ($\lambda_{exc} = 440$ nm) (△). The concentration of Re(I) chromophore was $[Re(I)] \approx 1.4 \times 10^{-3}$ M ($\lambda_{exc} = 440$ nm) (●) in experiments with $Fe^{III}(EDTA)^-$. A plot of the first derivative of the Stern−Volmer plot for the quenching of the luminescence of IV by the EDTA complexes is shown in panel b. The curves in panel b show the dependence of the Stern−Volmer constant, K_{SV}, on the quencher concentration.

concentration equal to or less than 4.2×10^{-3} M. Figure 5a shows nonlinear Stern−Volmer graphs, when the luminescence of IV was quenched with EDTA complexes of Cu(II) or Fe(III) in deaerated 50% v/v CH_3CN in an H_2O mixed solvent with a pH ~9. The slope of these plots (i.e., the Stern−Volmer constant, K_{SV}) decreased rapidly with quencher concentration and approached a constant value, $K_{SV} \approx 2.7 \times 10^3$ M^{-1} (Figure 5b).

The reactions between the quencher and the excited states of the polymer were investigated by flash photolyzing

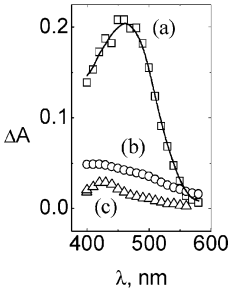

Figure 6. Transient spectra generated in 351 nm flash irradiations of V in deaerated 50% v/v CH_3CN in H_2O containing 6.0×10^{-4} M EDTA complexes. A spectrum recorded with a 15 ns delay from the laser irradiation (a) corresponds to the spectrum of the ^{3}MLCT excited state of the Re(I) chromophoress. The spectra recorded with a 250 ns delay from the laser irradiation correspond to the products of the reaction of the excited states with $Cu(EDTA)^{2-}$ (b) or $Fe^{III}(EDTA)^-$ (c).

solutions of polymer and quencher in 50% v/v CH_3CN in H_2O at 351 nm. Flash irradiations of V containing 3.0×10^{-3} or 6.0×10^{-4} M $Cu^{II}(EDTA)^{2-}$ produced a prompt transient spectrum identified as the ^{3}MLCT spectrum of the chromophores (panel a in Figure 6). The conversion of this spectrum into the spectrum of the product occurred via a first-order process whose lifetime was independent of the quencher concentration. Rate constants, $k = (2.40 \pm 0.04) \times 10^7$ s^{-1} and $(2.37 \pm 0.04) \times 10^7$ s^{-1}, were calculated from the traces recorded at 450 nm with 6.0×10^{-4} and 3.0×10^{-3} M concentrations of $Cu^{II}(EDTA)^{2-}$, respectively. The product of the reaction between the chromophores' ^{3}MLCT and $Cu^{II}(EDTA)^{2-}$ (Figure 6b), has an absorption band where it is expected, based on literature reports,[14,22] for the Re(II) chromophores (i.e., $\lambda_{max} \approx 480$ nm). The decay of the Re(II) product spectrum occurs by a process that is kinetically second order. The ratio of the rate constant to the extinction coefficient, $k/\epsilon = (1.15 \pm 0.04) \times 10^8$ cm s^{-1}, was calculated from the oscillographic traces recorded at 450 nm. A back electron-transfer reaction between the oxidized Re(II) chromophores and $Cu^{I}(EDTA)^{3-}$ (i.e., a reaction returning the polymer's chromophores and the quencher to their prephotolysis oxidation state) accounts for the observed reaction. Similar experimental observations were made when $Fe^{III}(EDTA)^-$ was used as a quencher of the excited chromophores instead of $Cu^{II}(EDTA)^{2-}$. The ^{3}MLCT spectrum of the chromophores decayed via a process that was kinetically first order in ^{3}MLCT concentration and with a lifetime independent of the $Fe^{III}(EDTA)^-$ concentration, $1/\tau = (4.19 \pm 0.04) \times 10^7$ s^{-1} at $\lambda_{ob} = 450$ nm. In addition, the spectrum of the product observed after the decay of the ^{3}MLCT (panel b in Figure 6) decayed on a longer time scale through a process with a second-order kinetics, $k/\epsilon = (6.20 \pm 0.04) \times 10^7$ cm s^{-1} at $\lambda_{ob} = 480$ nm.

In contrast to the oxidative reactions of the Fe(III) and Cu(II) EDTA complexes with the ^{3}MLCT excited states of the Re(I) chromophores, $Fe(CN)_6^{4-}$ quenches the luminescence of IV and V by reductive electron-transfer reactions. Transient spectra were recorded in the flash irradiations ($\lambda_{exc} = 351$ nm) of IV or V in 50% v/v CH_3CN in H_2O containing 2.0×10^{-5} M $Fe(CN)_6$.$^{4-}$ Such spectra revealed the formation of a product after the decay of the spectrum of the ^{3}MLCT excited state on a 250 ns time scale. The spectrum of the product was the same as that recorded for the reduction of IV and V by pulse radiolytically generated radicals, and it decayed through a process with second-order kinetics. A ratio of the rate constant to the extinction coefficient, $k/\epsilon = 1.7 \pm 0.04 \times 10^8$ cm s^{-1}, was calculated from the decay of the absorbance at $\lambda_{ob} = 460$ nm. Little if any static quenching was observed when the $Fe(CN)_6^{4-}$ concentrations in solutions of IV or V were equal to or less than 3.0×10^{-5} M. The rates of decay of both components of the chromophores luminescence were accelerated by $Fe(CN)_6^{4-}$, and the corresponding rate constants exhibited a nonlinear dependence on the concentration of quencher. Such a dependence of the rate constant on the $Fe(CN)_6^{4-}$ concentration is consistent with the existence of chromophores in a diversity of environments, an observation discussed elsewhere in this work.

A slow process occurring after the reduction of electronically excited chromophores in V by 2,2′,2″-triethanolamine, TEOA, was identified as an electron-transfer reaction between chromophores. Indeed, the product of the 351 nm flash irradiation of V in CH_3CN containing 0.6 M TEOA has the spectrum of the $-Re^{I}(CO)_3(2,2'\text{-bpy}^{\bullet-})$ chromophore, Figure 7a. The spectrum changes on a time scale of 50−400 μs, and these spectral changes are in accordance with the formation of $-Re^{I}(CO)_3(phen^{\bullet-})$ chromophores.

Ground-State Reduction Products. The spectra of the products produced by the one-electron reduction of $-Re^{I}(CO)_3(phen)^+$- and $-Re^{I}(CO)_3(2,2'\text{-bpy})^+$-containing compounds was investigated by pulse radiolysis of their solutions in CH_3OH. The $-Re^{I}(CO)_3(phen)^+$ and $-Re^{I}(CO)_3(2,2'\text{-bpy})^+$ chromophores in concentrations of $[Re(I)] \approx 1.3 \times 10^{-4}$ M failed to react with the pulse radiolytically generated $C^{\bullet}H_2OH$ radicals. They were reduced however by e^-_{sol} with a diffusion-controlled rate. The spectra of the reduction products of I, $ClRe(CO)_3(2,2'\text{-bpy})$, and V are shown in Figure 7b. They are nearly the same spectra of the $phen^{\bullet-}$, $2,2'\text{-bpy}^{\bullet-}$, or both radicals coordinated to Re(I). A comparison of the spectra of the monomeric and polymeric Re(I) complexes in Figure 7b reveals that e^-_{sol} reduces the $-Re^{I}(CO)_3(phen)^+$ and $-Re^{I}(CO)_3(2,2'\text{-bpy})^+$ chromophores in V. An average molar relationship of ~65:1 $-Re^{I}(CO)_3(phen^{\bullet-})$ to $-Re^{I}(CO)_3(2,2'\text{-bpy}^{\bullet-})$ chromophores in the strand of the polymer was calculated by using the extinction coefficients of the coordinated radicals and the radiolytically induced spectral changes. This molar relationship is fairly disparate from the 1:1 molar relationship expected if the attack of the Re(I) pendants in the strand by e^-_{sol} is stochastically controlled.

Discussion

Morphology of the Re Polymers. Polymers IV and V, containing two different pendants in the strand (i.e., $-Re(CO)3(phen)^+$ and $-Re(CO)_3(2,2'\text{-bpy})^+$), form nanometric aggregates in solution phase. The bimodal relaxation time spectra recorded for polymers IV and V reveal the existence of particle sizes between 3 and 14 nm in equilibrium with

(22) Personal communication from Dr. P. Juliarena.

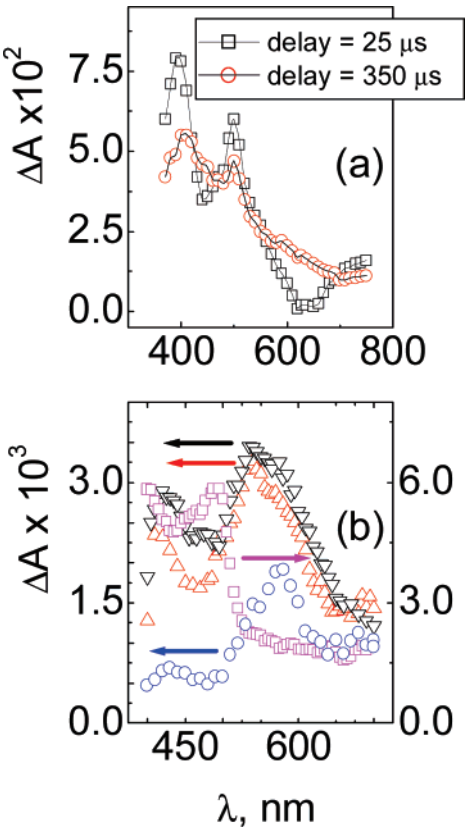

Figure 7. Spectra of the photolytically or radiolytically generated reduction products of Re(I) chromophores. The spectra of the products of the reduction of the excited state of V with TEOA are shown in panel a with two delays from the 351 nm laser irradiation. Deaerated solutions of the polymer in CH_3CN contained 0.6 M TEOA and concentrations of −Re(I) chromophores of [Re(I)] ≈ 1.0×10^{-4} M. The products of the reduction of $ClRe(CO)_3$(phen) (○), $ClRe(CO)_3$(2,2′-bpy) (□), IV (△), and I (▽) by pulse radiolytically generated e^-_{sol} are shown in panel b. Experimental conditions of the pulse radiolysis experiments are indicated elsewhere in the text.

bigger particles with radii between 40 and 300 nm. Given the hydrodynamic radius, 221 ± 9 nm for polymer IV with 294 ± 5 for polymer V, the aggregates must be bigger in polymer V than in polymer IV. We have previously observed aggregates of polymer II in acetonitrile solutions. It appears now that the larger the Re(I) load in the polymer, the bigger the size of the aggregates. TEM images obtained for polymers IV and V also show that the aggregates of the polymer V are larger than those of the polymer IV. Radii obtained from the DLS experiments are larger than those observed in the TEM micrographs. Similar differences were observed between the DLS hydrodynamic radii and those extracted from the TEM images of II. However, these differences in polymers IV and V are much larger, making the radii determined from TEM images a factor 2 smaller. Although these differences could be attributed to a solvent-induced swelling of the aggregate particles in solution phase, there are other factors which could also contribute, and they are currently being investigated.

Absorption Spectroscopy of Re(I) Pendants. Theoretical calculations in the literature have shown that two or three of the highest-occupied electronic levels in $XRe(CO)_3L$ complexes (L = phen or 2,2′-bpy and X = spectator ligand) correspond to orbitals largely centered in the Re.[23] Optically induced charge-transfer transitions from these orbitals to a LUMO, centered in the 2,2′-bpy or phen ligands, account for several absorption bands in the spectrum of the Re complexes (Table 1).[24,25] In a C_2 point-symmetry group, there are three MLCT electronic transitions (i.e., ^{1}MLCT(^{1}A′) ← ^{1}A′, ^{1}MLCT(^{1}A$_1$″) ← ^{1}A′, and ^{1}MLCT(^{1}A$_2$″) ← ^{1}A′).[23] Optical transitions promoting electrons between orbitals centered on the ligand 2,2′-bpy or phen occur at shorter wavelengths.

Two absorption bands, $\lambda_{max} \geq 365$ nm, in the absorption spectrum of monomeric and polymeric complexes containing $-Re^I(CO)_3(2,2'\text{-bpy})^+$, $-Re^I(CO)_3(phen)^+$, or both chromophores (Table 1 and Figure 2) have been related to optically induced charge-transfers from the Re to the 2,2′-bpy or phen ligands in the literature reports. The position of these bands vary from one compound to another because of the various contributions of the spectator ligand to the electronic structure, the interactions of the Re chromophore with the medium, and the nature of substituents in the acceptor ligand (i.e., a phen or 2,2′-bpy derivative). In general terms, the bands in the spectra of the polymeric compounds are blue shifted with respect to those of the monomers (Table 1). A rationale for the difference between the spectra of Re(I) chromophores in monomers and those in polymers is the existence of Re chromophores occupying different solvation spheres in the aggregates of polymer. Optically induced MLCT transitions occur at shorter wavelengths in those pendent chromophores placed in lesser-solvating environments than those of the monomeric Re(I) compounds. This proposition is consistent with the photochemistry of polymers IV and V discussed later in this work. A third absorption band, $\lambda_{max} = 350 \pm 10$ nm, is not a feature observed in the spectra of all the complexes in Table 1. Because of the position of the band in the spectrum and the magnitude of the extinction coefficient, the absorption band must have its origin in an optically induced charge-transfer transition from the Re to the 2,2′-bpy or phen ligands.

The position of the fourth band, $\lambda_{max} = 320 \pm 20$ nm in Table 1, is consistent with optically induced transitions from py groups to either 2,2′-bpy or phen ligands. Indeed, optically induced py to phen or 2,2′ -bpy charge-transfer transitions are expected at ∼320 nm. This assignment is based on the literature reduction potentials of the couple $py^{\cdot+}$/py, the acceptor reduction potentials, and the position, ∼ 390 nm, of the lowest-energy Re to phen or 2,2′-bpy charge-transfer transitions. It is not possible to ascertain if the py coordinated to Re or to the pendant py in the polymer backbone function as electron donors in the electronic transition. However, absorption bands in the spectra of $pyRe(CO)_3(phen)^+$ and I appear near the same wavelength, $\lambda_{max} = 325 \pm 3$ nm. This observation suggests that it is the py coordinated to Re in

(23) Ronco, S.; Ferraudi, G. In *Handbook of Photochemistry and Photobiology*; Nalwa, H. S., Ed.; American Scientific Publishers: Stevenson Ranch, CA, 2003; Vol. 1, Chapter 8, pp 316−318 and references therein.
(24) Hino, J. K.; Ciana, D. D.; Dressick, W. J.; Sullivan, P. S. *Inorg. Chem.* **1992**, *31*, 1072.
(25) Phillips, D. In *Polymer Photophysics*; Phillips, D., Ed.; Chapman and Hall: London, 1985; p 1.

Table 1. MLCT Absorption Bands in the UV−vis Spectrum of Monomeric and Polymeric Complexes in Acetonitrile

	λ/nm (ϵ/M^{-1} cm^{-1})			
pyRe(CO)$_3$(phen)$^+$	405 (7.9 × 10^2)	368 (3.4 × 10^3)	345 (4.1 × 10^3)	322 (6.4 × 10^3)
I[a]	390 (6.3 × 10^5)	365 (1.0 × 10^6)	350 (1.1 × 10^6)	328 (1.5 × 10^6)
pyRe(CO)$_3$(bpy)$^+$	378 (1.2 × 10^3)	354 (2.2 × 10^3)	317 (5.2 × 10^3)	304 (4.7 × 10^3)
(4-Etpy)Re(CO)$_3$(bpy)$^+$ [b]		348 (3.4 × 10^3)		
II[b]	362 (6.4 × 10^5)	342 (7.0 × 10^5)		319 (2.1 × 10^6)
IV	365 (7.2 × 10^5)	341 (8.5 × 10^5)		318 (1.8 × 10^6)
V	358 (1.6 × 10^6)	338 (1.8 × 10^6)		319 (3.9 × 10^6)
(4-Etpy)Re(CO)$_3$(bpy)$^+$				

[a] It additionally has a $\pi\pi^*$ transition at 263.4 nm. [b] Taken from ref 24. [c] It additionally has $\pi\pi^*$ transitions at ∼266.5 and 226.1 nm (complex bands).

the monomer and the polymer that is involved in the charge-transfer transitions. On this basis, the absorption bands at $\lambda_{max} = 320 \pm 20$ nm in the spectra of IV and V must be attributed to the set of ^{1}MLCT ← ^{1}A transitions discussed above and a ^{1}A ← ^{1}LLCT transition. The existence of LLCT electronic transitions in the pendants is supported by the known redox potentials of the ligands coordinated to Re(I) and the estimated reorganization energies. Moreover, LLCT electronic transitions have been assigned in the spectrum of related Re(I) complexes with derivatives of pyridine.

Luminescence of the Re(I) Pendants. Polymers IV and V have the same luminescence spectrum after normalization with respect to the maximum intensity of the emission, and it displayed a strong resemblance with the emission spectrum of I (Figure 2a). There are, however, some small differences between the spectrum of I and the spectra of IV and V. Such differences can be attributed to a small contribution from the emission of the $-Re^I(CO)_3(2,2'\text{-bpy})^+$ chromophores to the emission spectrum of IV and V. The excitation spectrum in Figure 2b suggests conversion of the high-energy excited states to the lowest-energy MLCT with various efficiencies. Maxima at $\lambda_{exc} \approx 390$, 338, and 316 nm in the excitation spectra of IV and V can be correlated with three MLCT absorption bands (i.e., bands positioned at $\lambda \geq 310$ nm in the absorption spectrum of the polymers, Table 1). Given the independence of the emission spectrum on the excitation wavelength, the excitation spectrum in Figure 2b reveals an efficient conversion to the luminescent triplet MLCT excited states, ^{3}MLCT, of those excited states populated when IV and V are irradiated at wavelengths of $325 \leq \lambda_{exc} \leq 420$ nm. In contrast to the latter MLCT excited states, the ^{1}IL and ^{1}LLCT excited states populated by the irradiation with light of a shorter wavelength than 320 nm convert with a lesser efficiency to the luminescent ^{3}MLCT excited states.

A manifestation of the various environments where Re(I) chromophores of IV and V are placed is the dependence of $k_1 = 1/\tau_1$ on λ_{ob} (Figure 4) and the lack of linearity in Stern−Volmer plots (Figure 5).[25−27] These experimental observations account for the presence of medium-destabilized charge-transfer excited states, (^{3}MLCT$_i$)P, in some chromophores within a strand of polymer.[23] (^{3}MLCT$_i$)P excited states decay to the ground state, or they transfer energy to other chromophores where medium-stabilized charge-transfer

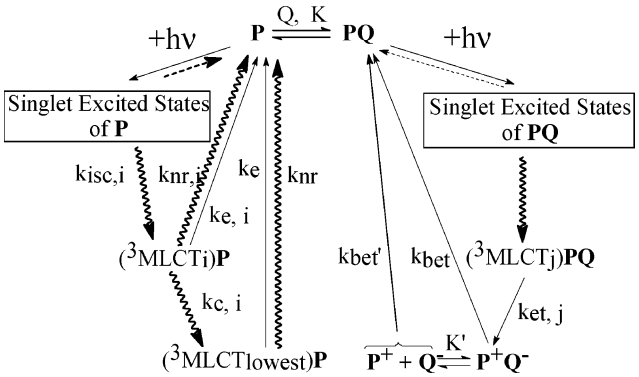

Figure 8. Flowchart showing the relevant photophysical processes in IV and V (left side) and the static quenching of the charge-transfer excited states by EDTA complexes (right side). The polymer aggregates are represented by P and their adducts with the EDTA complexes by PQ. The environment-destabilized MLCT excited states of Re(I) chromophores have been identified with subscripts i and j. The rate constants of the various processes have been defined elsewhere in the text.

excited states (^{3}MLCT$_{lowest}$)P, are produced (Figure 8). The rate constant for the decay of the (^{3}MLCT$_i$)P, $k_{decay,i}$, has been expressed, $k_{decay,i} = k_{e,i} + k_{nr,i} + k_{c,i}$, where $k_{e,i}$ is the rate constant for the radiative relaxation, $k_{nr,i}$ is the rate constant for the radiationless relaxation to the ground state, and $k_{c,i}$ is the rate constant for the conversion of the (^{3}MLCT$_i$)P to the (^{3}MLCT$_{lowest}$)P. On this basis, the integrated rate law for the (^{3}MLCT$_i$)P is

$$[(^3\text{MLCT}_i)\text{P}] = [(^3\text{MLCT}_i)\text{P}]_0 \exp -(k_{decay,i}t) \qquad (5)$$

where $[(^3\text{MLCT}_i)\text{P}]_0$ is the concentration of the (^{3}MLCT$_i$)P excited state at $t = 0$ (i.e., immediately after intersystem crossing processes produce the nonthermally equilibrated ensemble of triplet states). The integrated rate law of the (^{3}MLCT$_{lowest}$)P is obtained in the same manner (eq 6).

$$[(^3\text{MLCT}_{lowest})\text{P}] = \sum_i [(^3\text{MLCT}_i)\text{P}]_0 \frac{k_{c,i}}{k_{decay,L} - k_{decay,i}} (\exp - (k_{decay,i}t) - \exp -(k_{decay,L}t)) + [(^3\text{MLCT}_{lowest})\text{P}]_0 \exp - (k_{decay,L}t) \qquad (6)$$

In eq 3, $[(^3\text{MLCT}_{lowest})\text{P}]_0$ is the concentration of (^{3}MLCT$_{lowest}$)P at the same time when the set of excited states (^{3}MLCT$_i$)P achieved concentrations of $[(^3\text{MLCT}_i)\text{P}]_0$. Equations 5 and 6 were used in the respective expressions of the intensity of the luminescence (eq 7).

(26) Webber, S. C. In *Polymer Photophysics*; Phillips, D., Ed.; Chapman and Hall: London, 1985; p 41.
(27) Roberts, A. J.; Soutar, L. In *Polymer Photophysics*; Phillips, D., Ed.; Chapman and Hall: London, 1985; p 221.

$$I_{\text{emission}} = \sum_i \left(k_{e,i} - k_{e,L} \frac{k_{c,i}}{k_{\text{decay},i} - k_{\text{decay,L}}} \right) [(^3\text{MLCT}_i)\text{P}]_0 \exp -(k_{\text{decay},i} t) + k_{e,L} \left[\left(\sum_i [(^3\text{MLCT}_i)\text{P}]_0 \frac{k_{c,i}}{k_{\text{decay},i} - k_{\text{decay,L}}} \right) + [(^3\text{MLCT}_{\text{lowest}})\text{P}]_0 \right] \exp -(k_{\text{decay,L}} t) \quad (7)$$

One experimental observation is that the oscillographic traces of the luminescence decay were fitted to a biexponential function with positive preexponential factors. Therefore, a majority of the terms in eq 7 must obey the inequalities

$$\sum_i \left(k_{e,i} - k_{e,L} \frac{k_{c,i}}{k_{\text{decay},i} - k_{\text{decay,L}}} \right) > 0$$

$$\left(\sum_i [(^3\text{MLCT}_i)\text{P}]_0 \frac{k_{c,i}}{k_{\text{decay},i} - k_{\text{decay,L}}} \right) + [(^3\text{MLCT}_{\text{lowest}})\text{P}]_0 > 0$$

The rate constants $k_{\text{decay},i}$ and $k_{\text{decay,L}}$ can be associated with processes whose average lifetimes are $\tau_1 \approx 10^{-7}$ s and $\tau_2 \approx 10^{-6}$ s, respectively (i.e., the two sets of lifetimes calculated from the oscillographic traces of the absorbance or emission decays). On this basis, it must be $k_{\text{decay},i} - k_{\text{decay,L}} > 0$ in the significant terms of eq 7. Since the second component of the emission is observed with $1/\tau_2 \approx 10^6$ s^{-1}, $k_{e,L}$ must have a significant value but $k_{\text{decay},i} - k_{\text{decay,L}} \approx k_{\text{decay},i}$ remains a valid approximation. In this approximation, $k_{c,i}/k_{\text{decay},i}$ could be the dampening factor (i.e., $k_{c,i}/k_{\text{decay},i} < 1$), and eq 7 can be reduced to eq 8.

$$I_{\text{emission}} = \sum_i (k_{e,i} [(^3\text{MLCT}_i)\text{P}]_0 \exp -(k_{\text{decay},i} t) + k_{e,L} \left[\left(\sum_i [(^3\text{MLCT}_i)\text{P}]_0 \frac{k_{c,i}}{k_{\text{decay},i}} \right) + [(^3\text{MLCT}_{\text{lowest}})\text{P}]_0 \right] \exp -(t/\tau_2) \quad (8)$$

Equations 2 and 3 were also used to deduce the expression of the absorbance change in flash photolysis (eq 9). Because

$$\Delta A = \sum_i \left(\left(\epsilon_i - \epsilon_L \frac{k_{c,i}}{k_{\text{decay},i}} - \epsilon_{GS} \right) [(^3\text{MLCT}_i)\text{P}]_0 \exp -(k_{\text{decay},i} t) \right) + (\epsilon_L - \epsilon_{GS}) \left[\left(\sum_i [(^3\text{MLCT}_i)\text{P}]_0 \frac{k_{c,i}}{k_{\text{decay},i}} \right) + [(^3\text{MLCT}_{\text{lowest}})\text{P}]_0 \right] \exp -(t/\tau_2) \quad (9)$$

each term under the first summation in eqs 8 and 9 has an intrinsic lifetime, $1/k_{\text{decay},i}$, the lifetimes calculated for the faster component in the decay of the emission and ΔA exhibit a dependence on the monitoring wavelength, Figure 4. The experimental observations show that terms weighted by the extinction coefficients of the excited states, ϵ_i of $(^3\text{MLCT}_i)\text{P}$, in eq 6 must impart a stronger dependence of τ_1 on the monitoring wavelength than those weighted by $k_{e,i}$ in eq 8.

Ground and Excited-State Redox Reactions. The redox reactions of the $^3\text{MLCT}_{\text{lowest}}$ and $^3\text{MLCT}_i$ with the anionic Fe(III) and Cu(II) EDTA complexes have the kinetics expected for a static quenching of the luminescence (i.e., one caused by the formation of ground-state adducts PQ, Figure 8). Either or both the generation of $^3\text{MLCT}_i$ excited states decaying with different rates in the aggregates of polymer and different binding constants of the EDTA complexes to Re(I) chromophores in different environments account for the curvature of the Stern−Volmer plots, Figure 5. The products of the adducts' excited-state reactions are Re(II) pendants, P^+, which undergo back-electron-transfer reactions with the reduced EDTA complexes, Q^-. The second-order kinetics of the back-electron-transfer reactions suggests a sufficiently large dissociation of the P^+Q^- pairs in Figure 8b to make the rate of the bimolecular process, $k_{\text{bet}}[\text{P}^+][\text{Q}^-]$, larger than the rate of the unimolecular process, $k_{\text{bet}}[\text{P}^+\text{Q}^-]$.

$Fe(CN)_6^{4-}$ or TEOA were oxidized when they reacted with the electronically excited chromophores. In contrast to the EDTA complexes, the kinetics of the reaction between the excited-state chromophores and $Fe(CN)_6^{4-}$ revealed little if any association between the counterions to provide the conditions for static quenching. Since $Fe(CN)_6^{4-}$ and the EDTA complexes are anions, electrostatic interactions cannot solely be the reason for the static quenching. A more plausible explanation for the static quenching of the EDTA complexes is that the electrostatic interactions operate jointly with coordination of the EDTA complexes to the py pendants. In the polymer, the metal ions of the EDTA complexes can be coordinated to the py pendants using those positions of the coordination sphere otherwise occupied by solvent molecules. No coordination of the py pendants to the substitution inert $Fe(CN)_6^{4-}$ is possible, and the reaction of this complex with the excited states is therefore a dynamic process.

When TEOA reacts with the MLCT excited states, the cationic radicals, $(HOCH_2CH_2)_3N^{\bullet+}$, do not undergo back-electron-transfer reactions with the reduced Re(I) pendants. The absence of a back-electron-transfer reaction suggests that the rate of this reaction is greatly reduced by the repulsive electrostatic interaction between the cationic radicals and the electrostatic field of the polyelectrolyte.

Because the retardation of the back-electron-transfer reaction, intrastrand electron-transfer processes of the reduced chromophores have been observed in pulse radiolytic and flah photochemical experiments at a longer time scale. These redox processes allow the $-\text{Re}^{\text{I}}(\text{CO})_3(2,2'\text{-bpy}^{\bullet-})$ and $-\text{Re}^{\text{I}}(\text{CO})_3(\text{phen}^{\bullet-})$ chromophores to achieve thermal equilibrium in accordance with their chemical potentials. There is a resemblance between the intrastrand processes driving the $-\text{Re}^{\text{I}}(\text{CO})_3(2,2'\text{-bpy}^{\bullet-})$ and $-\text{Re}^{\text{I}}(\text{CO})_3(\text{phen}^{\bullet-})$ populations to such a thermal equilibrium and electron-exchange reactions whose driving force is $\Delta G^\circ \approx 0$.

Acknowledgment. G.F. acknowledge support from the Office of Basic Energy Sciences of the U.S. Department of Energy. This is Contribution NDRL-4592 from the Notre Dame Radiation Laboratory. E.W. and M.F. acknowledge Grant PICT 06-12610 from ANPCyT and CONICET-PIP 02470/00 from the Consejo Nacional de Investigaciones Cientificas y Tecnológicas (Universidad Nacional de La Plata) and CICPBA.

Supporting Information Available: Figure 1S with typical NMR spectra of monomer and polymer Re compounds, Figure 2S showing the relaxation time distribution, *L* (ln) versus time, and Table 1S with normalized electric field time correlation functions (TCF) and standard deviations (SD) of three representative samples. This material is available free of charge via the Internet at http://pubs.acs.org.

IC060266S